RSC Advances

This article can be cited before page numbers have been issued, to do this please use: C. P. Sen and S. Valiyaveettil, *RSC Adv.*, 2016, DOI: 10.1039/C6RA21348K.

ROYAL SOCIETY OF CHEMISTRY

www.rsc.org/advances

View Article Online
DOI: 10.1039/C6RA21348K

Journal Name

ARTICLE

Solvent Dependent Isomerization of Photochromic Dithienylethenes: Synthesis, Photochromism, and Self-assembly

Received 00th January 20xx,
Accepted 00th January 20xx

DOI: 10.1039/x0xx00000x

www.rsc.org/

Choong Ping Sen, and Suresh Valiyaveettil*

A series of photochromic dithienylethene incorporated with phenol (**DTE1**), catechol (**DTE2**), azophenol (**DTE3**) groups was synthesized and characterized by means of NMR spectroscopy, mass spectrometry and elemental analysis. The photophysical, photochromic and photoisomerization properties of molecules were studied using absorption and emission spectroscopies in different solvents. The *cis-trans* photoisomerizations of azophenols in **DTE3** compete with photocyclization of dithienylethene, resulting in low photoconversion yields in **DTE3**. Thermal isomerization of *cis*-azophenols was found to be solvent-dependent – a fast thermal relaxation from *cis*- to *trans*- isomer in chloroform, and a slow process in THF. For example in chloroform, formation of a closed-ring dithienylethene with *trans*- azophenols (*trans*-**DTE3**$_{closed}$) was observed upon irradiation with UV light (365 nm). On the other hand, closed-ring dithienylethene with *cis*-azophenols (*cis*-**DTE3**$_{closed}$) was formed in THF under the same condition. After forming a complex with Fe^{3+} ions, **DTE2** showed a red shift of 27 nm in the absorption maximum. Scanning electron microscopy (SEM) analysis revealed formation of circular nanostructures with diameters in the range of 300 – 600 nm from **DTE2**$_{closed}$ film. Factors such as solvent, photoisomerization, and hydrogen bonding toward the formation of such supramolecular nanostructures and morphologies are discussed.

Introduction

Photoinduced changes in chemical and physical properties of molecules have attracted great attention owing to potential applications in sensor,[1, 2] optical data processing[3] and molecular switches.[4] For example, azobenzene derivatives have been used extensively as photoresponsive system owing to the easy switchability of azobenzene, where *trans*-isomer can be switched to the *cis*-isomer by irradiation at around 340 nm and back to *trans*-isomer either by heating or by irradiation at around 450 nm.[5] The photoisomerization properties and kinetics have been well-established by varying the electron-withdrawing or electron-donating substituents on the azobenzene moiety.[6-8] The azophenolic derivatives with push-pull effects were reported to undergo fast *cis*-to-*trans* thermal relaxation within microseconds, which is useful for high speed optical oscillators.[9] On the other hand, considerable interests have also been focused on dithienylethene derivatives, which showed fast and stable photoinduced cyclization and cycloreversion, fatigue resistance, and high thermal stabilities of open and closed isomeric forms.[10-13] Therefore, it is interesting to study the effect of azophenol group on the overall photochromic properties of the system when the azophenol group is conjugated to the dithienylethene. Studies have shown that the azo group (non-conjugated to dithienylethene) significantly accelerated the ring-opening process of dithienylethene.[14, 15]

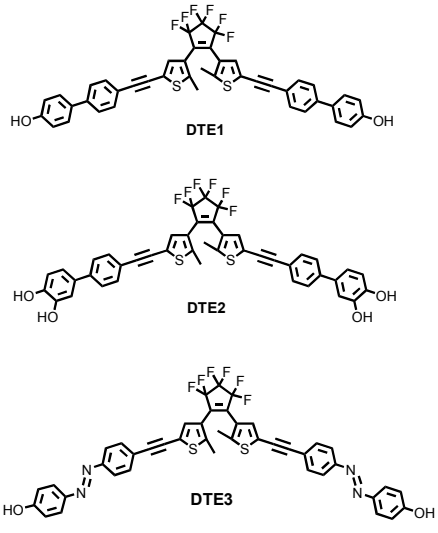

Figure 1. Chemical structures of dithienylethene with phenolic (**DTE1** - **DTE2**) and azophenolic (**DTE3**) end groups.

Department of Chemistry, 3 Science Drive 3, National University of Singapore, Singapore-117543.
**E-mail: chmsv@nus.edu.sg*

Electronic Supplementary Information (ESI) available: [^{1}H and ^{13}C NMR spectra, mass spectra, absorption and photoluminescence spectra, and SEM images of all compounds]. See DOI: 10.1039/x0xx00000x

View Article Online
DOI: 10.1039/C6RA21348K

In addition, hydrogen bonding and π-π interaction are known for directing self-assembly of the molecules into well-defined macrostructures. Recently, the self-assembly of DTE derivatives was investigated to show interesting supramolecular architectures such as helical fibrous microstructures,[16, 17] microspheres,[18] and flakes.[19, 20] In view of these, two photochromic dithienylethene molecules incorporated with end phenolic groups (**DTE1 - 2**) and another dithienylethene molecule incorporated with end azophenolic group (**DTE3**) were synthesized and the properties of all three molecules are compared (Figure 1). A detailed investigation of photoisomerization, electrochemistry, and self-assembly of all target molecules are carried out. Here, the roles of hydrogen bonding, azogroups, and photoisomerization toward formation of final self-assembled architecture of molecules are studied.

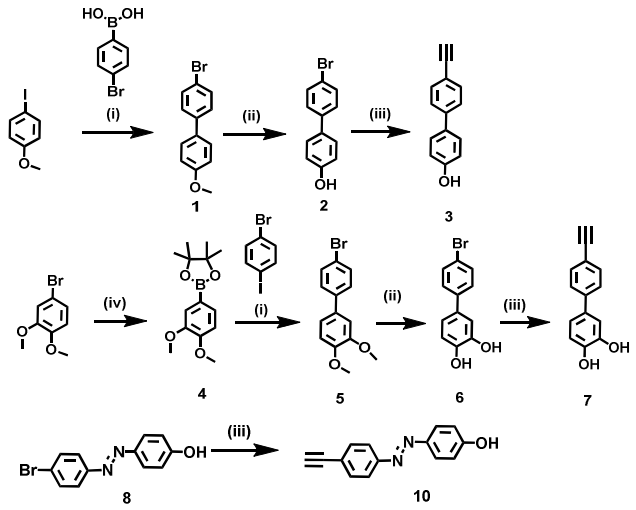

Scheme 1. Synthetic approach to obtain compound **3**, **7**, and **10**; (i) $PdCl_2(PPh_3)_2$, THF/Aliquat® 336/aqueous 2M K_2CO_3 solution, reflux, overnight, 83% (**1**); 79% (**5**); (ii) BBr_3, DCM, -50 °C to r.t., 3 hrs, 90% (**2**); 84% (**6**) (iii) (a) ethynyltrimethylsilane, $Pd(PPh_3)_4$, CuI, THF/TEA, 80 °C, 24 hrs, (b) TBAF, THF, °0 C, 30 mins, 80% (**3**), 69% (**7**), 81% (**10**); (iv) $PdCl_2$(dppf), bis(pinacolatodiboron), KOAc, 1,4-dioxane, 80 °C, overnight, 85%.

Results and Discussion

Synthesis of Target Molecules

Synthetic routes for the target molecules, **DTE1**, **DTE2**, and **DTE3** are given in Schemes 1 and 2. The biphenyl molecule with methoxy (compound **1**) group was obtained from Suzuki-Miyaura coupling reaction[21] between 4-iodoanisole and 4-bromophenylboronic acid in 83% yield. Similarly, the coupling between 1-bromo-4-iodobenzene and compound **4** afforded dimethoxy biphenyl bromide (compound **5**) in 79% yield. Demethylations of compound **1** and **5** were carried out using boron tribromide in anhydrous dichloromethane to afford compounds **2** and **6** in 90% and 84% yield, respectively. The bromine substituent on biphenyl compounds (**2** and **6**) or azophenol (**8**) was replaced with ethynylene group in two steps (69 – 81% yields); a palladium-catalyzed Sonogashira cross-coupling reaction[22] with ethynyltrimethylsilane, followed by desilylation using tetrabutylammonium fluoride. The corresponding desilylated compounds (**3**, **7**, and **10**) were reacted with iodinated dithienylperfluorocyclopentene (**DTE**) via Sonogashira coupling in presence of $Pd(PPh_3)_4$ and CuI as catalysts in tetrahydrofuran/diisopropylamine (2 : 1) as solvent mixture to afford the **DTEs** (34% - 79% yields). All intermediates and products were characterized fully using NMR spectroscopy, mass spectrometry, and elemental analyses (ESI, Figure S1 – S33). All **DTEs** are soluble in common organic solvents such as chloroform, toluene, acetonitrile, methanol and tetrahydrofuran.

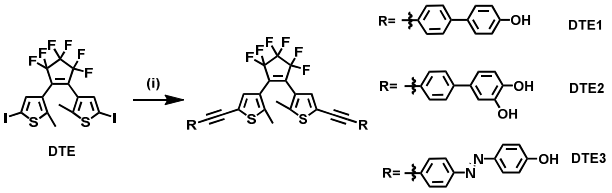

Scheme 2. Sonogashira reaction condition for **DTE1 - 3;** (i) $Pd(PPh_3)_4$, CuI, THF/DIPA, reflux, overnight, 49% (**DTE1**), 34% (**DTE2**), and 79% (**DTE3**).

Photochromic Properties of DTE1 and DTE2

The photochromic properties of **DTEs** were investigated using the absorption and emission spectroscopies (Figure 2). The absorption maxima of $\mathbf{DTE1}_{open}$ and $\mathbf{DTE2}_{open}$ (open-ring isomers) were observed at 328 nm in chloroform and showed red-shifts in absorption maximum (λ_{max} = 332 - 336 nm) when dissolved in THF (Figure 3).[23] $\mathbf{DTE2}_{open}$ with catechol group exhibits an absorption maximum at longer wavelength (λ_{max} = 336 nm) than that of $\mathbf{DTE1}_{open}$ (λ_{max} = 332 nm) in THF. Similarly, red-shifts in emission peaks were observed for $\mathbf{DTE1}_{open}$ (λ_{ems} = 390 nm and 412 nm) and $\mathbf{DTE2}_{open}$ (λ_{ems} = 416 nm) in THF in comparison to that in chloroform (λ_{ems} for $\mathbf{DTE1}_{open}$= 382 nm and 406 nm; for $\mathbf{DTE2}_{open}$ = 388 nm and 410 nm).

Formation of $\mathbf{DTE1}_{closed}$ and $\mathbf{DTE2}_{closed}$ isomers was observed with appearance of a new absorption maximum at around 620 nm, and two low-energy absorption maxima (within the ranges of 368 – 372 nm; and 287 - 300 nm) upon irradiation with UV-light (at 365 nm, 5 minutes) in chloroform or THF. The colorless **DTE1 - 2**$_{open}$ solutions changed to dark-blue upon reaching a photostationary state. The three absorption peaks are assigned to the $S_0 – S_1$ (620 nm), $S_0 – S_2$ (325 – 372 nm), and $S_0 – S_3$ (287 – 300 nm) transitions of **DTE1 - 2**$_{closed}$.[24]

View Article Online
DOI: 10.1039/C6RA21348K

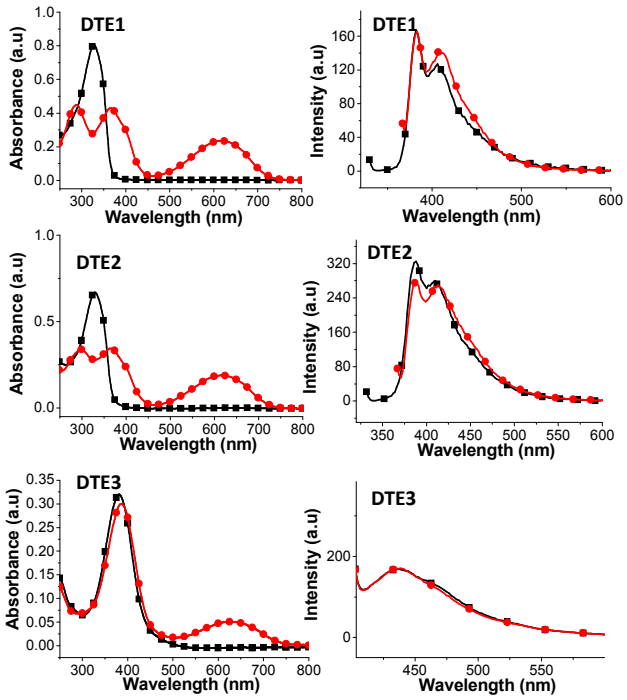

Figure 2. Absorption (left) and emission spectra (right) of **DTEs** in chloroform; open-ring isomer (-■-) and closed-ring isomer (-●-) at photostationary state upon irradiation at 365 nm for 5 minutes.

DTE1$_{closed}$ showed a broadened absorption peak with insignificant changes in absorption maximum from THF to chloroform, which indicated a minimal solvent-dependent effect on its electronic property. On the other hand, **DTE2**$_{closed}$ exhibited a significant blue-shift in $S_0 - S_2$ transition (λ_{max} = 325 nm) in THF as compared to that in chloroform (λ_{max} = 366 nm), suggesting a stronger solvent effect on the electronic property of **DTE2**$_{closed}$. The fluorescence quantum yield of **DTE1 – 2** decreased with changes in solvent from chloroform to MeOH, as a result of the photoinduced electron transfer in polar solvent.[12]

^{1}H NMR analyses were carried out to calculate the photoconversion yields of **DTE1 - 2**$_{open}$ at photostationary states (ESI, Figure S34 – 35). For example, the chemical shift of methyl groups at the bridge carbon for **DTE1**$_{closed}$ was shifted downfield to 2.22 ppm compared to the one found in **DTE1**$_{open}$ (2.00 ppm). Moreover, the thienyl proton of ring-closed isomer had shifted upfield to 6.53 ppm from 7.28 ppm. Based on the NMR integration, **DTE1**$_{open}$ and **DTE2**$_{open}$ showed similar photoconversion yields of 70% and 74%, respectively, at photostationary states. The cyclization (ϕ_{o-c}) and cycloreversion (ϕ_{c-o}) quantum yields of **DTEs** were estimated by comparing the initial reaction yields with the known yield of the compound, 1,2-bis(2-methyl-5-phenyl-3-thienyl)perfluorocyclopentene.[25, 26] Similar cyclization quantum yields were obtained for **DTE1**$_{open}$ (ϕ_{o-c} = 0.28) and **DTE2**$_{open}$ (ϕ_{o-c} = 0.26). On the other hand, smaller cycloreversion quantum yields were observed for **DTE1**$_{closed}$ (ϕ_{c-o} = 0.0031) and **DTE2**$_{closed}$ (ϕ_{c-o} = 0.0025).

The **DTE1**$_{open}$ and **DTE2**$_{open}$ thin films were prepared from chloroform solutions (ESI, Figure S38). Photoisomerizations of **DTE1**$_{open}$ and **DTE2**$_{open}$ were carried out by exposing the thin films under UV-light for 5 minutes. In general, the absorption maxima of thin films of **DTE1 – 2**$_{open}$ and **DTE1 – 2**$_{closed}$ showed significant red-shift than those in chloroform solutions, and were similar to the values observed in THF solutions. For example, thin films of **DTE2**$_{open}$ showed absorption maxima at 336 nm, as compared to that in chloroform solution (λ_{max} = 328 nm) and in THF solution (λ_{max} = 332 nm). Similarly, **DTE2**$_{closed}$ thin film showed two absorption maxima at 323 nm and 624 nm, as compared to that in chloroform solution (λ_{max} = 296 nm, 620 nm) and in THF solution (λ_{max} = 325 nm, 624 nm).

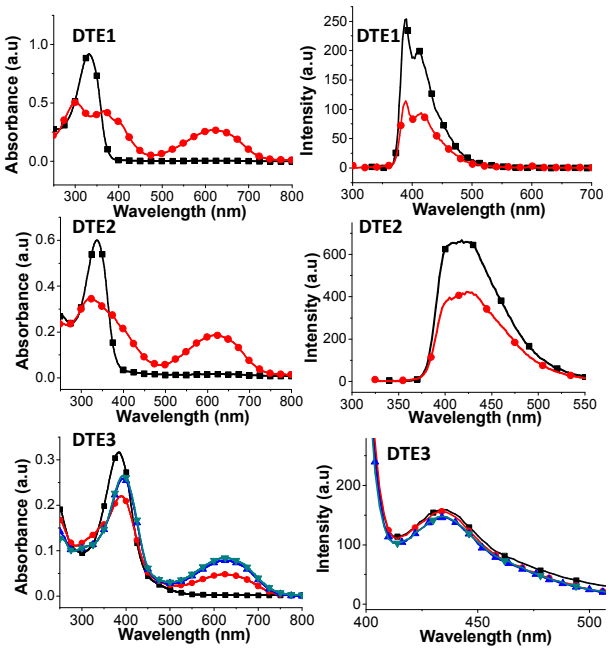

Figure 3. Absorption (left) and emission spectra (right) of **DTEs** in THF for open-ring isomer (-■-) and closed-ring isomer (-●-) at photostationary state upon irradiation at 365 nm for 5 minutes; for **DTE3**, the absorption and emission spectra of open-ring isomer (-■-) after irradiation at 365 nm for 1 minute (-●-), 3 minutes (-▲-), and 5 minutes (-▼-) are shown.

Photochromic Properties of DTE3 in chloroform

The photochromic properties of **DTE3** incorporated with dithienylethene and azophenol units were studied in chloroform (Figure 2). The orange colored solutions of **DTE3**$_{open}$ in chloroform gradually turned into green upon irradiation with UV-light for 15 minutes. The appearance of new absorption peak at 630 nm indicates formation of **DTE3**$_{closed}$. The photophysical properties of **DTEs** are summarized in Table 1.

View Article Online
DOI: 10.1039/C6RA21348K

Table 1. Summary of photophysical properties of **DTEs** in different solvents.

	$CHCl_3$		THF		MeOH		Thin Film
	λ_{max} [a], nm	λ_{ems} [a], nm (ϕ_f [c], %)	λ_{max} [a], nm	λ_{ems} [a], nm (ϕ_f [c], %)	λ_{max} [a], nm	λ_{ems} [a], nm (ϕ_f [c], %)	λ_{max} [b], nm
DTE1$_{open}$	328	382, 406 (15.3)	332	390, 412 (13.2)	332	410 (10.4)	330
DTE1$_{closed}$	287, 368, 620	382, 410 (16.1)	300, 372, 620	390, 415 (8.6)	296, 360, 615	410 (6.3)	295, 374, 624
DTE2$_{open}$	328	388, 410 (12.4)	336	416 (9.8)	335	453 (7.1)	336
DTE2$_{closed}$	296, 366, 620	388, 412 (13.9)	325, 624	419 (6.7)	311, 610	455 (5.6)	323, 624
DTE3$_{open}$	382	437 (8.7)	384	437 (6.5)	381	434 (5.4)	379
DTE3$_{closed}$	387, 630	437 (8.5)	393, 630	437 (5.9)	386, 615	441 (3.9)	642

[a] Absorption maxima and emission peak were measured in dilute solution. [b] Thin films were prepared by dropcasting the solution of molecules onto quartz plates, followed by slow evaporation at room temperature. [c] Fluorescence quantum yields were estimated by using quinine sulfate in 0.5 M H_2SO_4 as reference.[27]

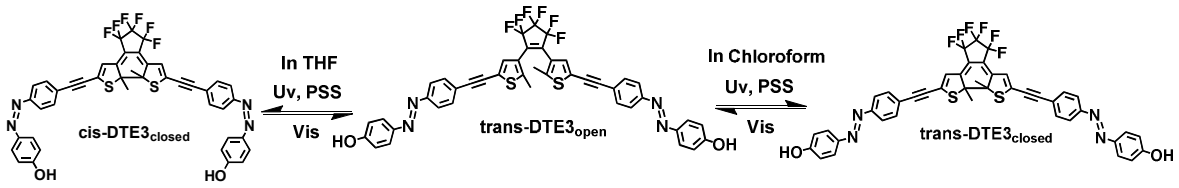

Scheme 3. DTE3 isomers in THF and chloroform at photostationary state (PSS).

The small decrease in intensity of absorption at 382 nm for **DTE3**$_{closed}$ after irradiation suggests that the azophenol groups in **DTE3**$_{closed}$ molecules are in *trans*- form. In addition, the ^{1}H NMR analysis showed no changes in chemical shifts for trans-azophenol groups at photostationary state. Moreover, the integration of ^{1}H NMR signals showed low photoconversion yields of 32% for **DTE3** (ESI, Figure S36), which is explained as the energy loss from fast thermal relaxation in azophenols. The cyclization and cycloreversion quantum yields of **DTE3** in chloroform were estimated to be 0.09 and 0.0011, respectively, which are smaller than that observed for **DTE1** and **DTE2**.

Photochromic Properties of DTE3 in THF and in Thin Film

The THF solution of **DTE3**$_{open}$ showed a fast decrease in absorbance at 384 nm and appearance of absorption peak at 630 nm (Figure 3) upon irradiation with UV-light for one minute, which is different from **DTE3**$_{open}$ in chloroform. This indicates that **DTE3**$_{closed}$ has both ring-closed dithienylethene and *cis*-azophenols in THF (Scheme 3).

The photoisomerization can be switched reversibly and the increase in absorbance (Abs) at 630 nm was observed for **DTE3**$_{closed}$ in THF (Abs = 0.09) as compared to that obtained in chloroform (Abs = 0.05), indicating a higher photoconversion yield at the photostationary state in THF. The yield of photoinduced ring closing of the dithienylethene and trans-cis isomerization of **DTE3** are ~48% and ~62%, respectively, at photostationary state (ESI, Figure S37). The presence of additional NMR peaks suggests the formation of **DTE3** isomer with open-ring dithienylethene and cis-azophenol groups. A sharp hydroxyl proton peak (9.03 ppm) was found for **DTE3** in deuterated THF, which indicates a slow proton exchange owing to the strong hydrogen bonding. This demonstrates that the stabilization of azophenols improves the photoconversion yield of dithienylethene. In addition, the cyclization and cycloreversion quantum yields of **DTE3** in THF were estimated to be 0.15 and 0.0021, respectively, which are higher than that in chloroform.

Thin films of **DTE3**$_{open}$ were prepared from solutions of compounds in chloroform and THF and the photochromic properties were investigated by spectroscopic techniques (Figure 4). Similar photochromic changes were observed for **DTE3**$_{open}$ upon irradiation with UV-light, where ring-closed dithienylethene and *cis*-azophenols were formed inside the films prepared from THF solution (Figure 4b). However, thermal relaxation of *cis*-azophenols happened after 30 minutes due to complete evaporation of THF from **DTE3**$_{open}$ film.

View Article Online
DOI: 10.1039/C6RA21348K

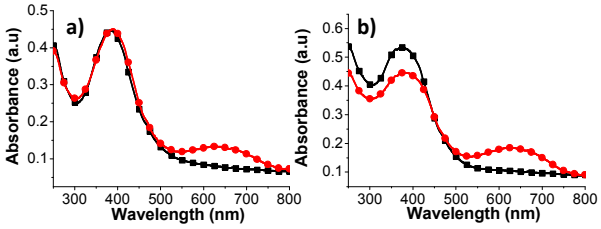

Figure 4. Normalized absorption spectra of **DTE3** films prepared from chloroform (**a**) and THF (**b**); open-ring isomer (-■-) and closed-ring isomer at photostationary state (-●-) upon irradiation at 365 nm for 5 minutes. The films were prepared by dropcasting the solution of **DTE3** onto a quartz plate, followed by evaporation at room temperature.

Comparison of Photochromic Properties of DTE3 with DTE1 – 2

DTE3 absorbs at longer wavelength (i.e. λ_{max} = 382 nm in chloroform) due to incorporation of azo- group with more extended conjugation as compared to **DTE1** (i.e. λ_{max} = 328 nm in chloroform) and **DTE2** (i.e. λ_{max} = 328 nm in chloroform). Similarly, **DTE3** showed red-shift in emission maximum (λ_{ems} = 437 nm) in chloroform and THF. However, **DTE2** showed a longer emission maximum (λ_{ems} = 455 nm) as compared to that of **DTE3** (λ_{ems} = 441 nm) in methanol, which is attributed to the strong hydrogen bond between methanol and **DTE2**. In comparison, **DTE3**$_{open}$ showed a relatively slower photoinduced ring closing reaction due to the energy loss from fast thermal relaxation in azophenolic groups.[9] Also, **DTE3** showed smaller fluorescence quantum yield (3.9% - 8.7%) as compared to **DTE1 – 2** in different solvents.

The thermal stabilities of closed-isomers of **DTEs** in chlorobenzene were monitored by measuring their absorbance decay at 620 – 630 nm at 100 °C under darkness (ESI, Figure S39). The cycloreversion process of closed-isomers of **DTEs** becomes faster at elevated temperature. It is found that **DTE1**$_{closed}$ has higher thermal stability as compared to **DTE2**$_{closed}$ and **DTE3**$_{closed}$. The half-life of **DTE1**$_{closed}$, **DTE2**$_{closed}$, and **DTE3**$_{closed}$ are estimated to be around 60 hours, 39 hours, and 46 hours, respectively, at 100 °C. On the other hand, the THF solution of **DTE3**$_{closed}$ showed cis-trans isomerization after 15 minutes at 50 °C with reappearance of absorption peak at 384 nm and negligible absorbance changes at 630 nm region (ESI, Figure S40). This indicates the cis-azophenol is less thermally stable than closed-dithienylethene for **DTE3**. In addition, the changes in absorbance of the chloroform solution of **DTEs** at 620 – 630 nm were monitored after alternate irradiation with UV- and visible light. All **DTEs** showed no significant absorbance decay up to 15 irradiation cycles, which suggests a good fatigue resistance for **DTEs**.

Photochromic Properties of Azophenolic Compound 10

In order to prove that the observed changes in absorption intensities of **DTE3** upon irradiation with UV-light was caused by the formation of *cis*-azophenol, photochromic properties of compound **10** in different solvents were examined. A dilute chloroform solution of **10** was monitored by absorption spectroscopy before and after irradiation at 365 nm (Figure 5a).

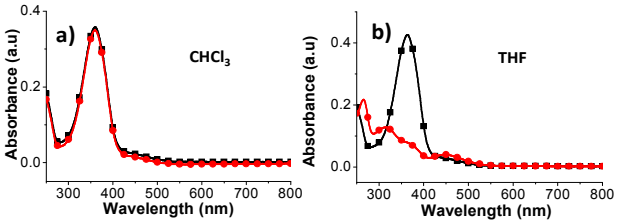

Figure 5. Absorption spectra of azophenolic compound, **10** in chloroform (**a**) and THF (**b**); *trans*- (-■-) and *cis*-isomer at the photostationary state (-●-) upon irradiation at 365 nm until no further changes in absorption profile.

The observed strong absorption maximum at 360 nm (π - π*) is consistent with the *trans*- form of **10**, and no changes in absorption profile was observed after irradiation (365 nm) for 10 minutes in chloroform. It was reported that the azobenzenes incorporated with phenol substituent showed fast thermal relaxation in milliseconds scale which is difficult to be detected at room temperature.[28] This is explained by the formation of hydrazine intermediate *via* intermolecular proton transfer between phenol and nitrogen atom of the azo group, which lowers the energy barrier of switching from *cis*-isomer to *trans*-isomer.[8] In contrast, the THF solution of **10** showed *trans-cis* conversion with a decrease in intensity of absorption maximum at 360 nm and appearance of a new absorption peak at 450 nm after irradiation (365 nm, 1 minute, Figure 5b).[29] The trans-isomer can be recovered by irradiating the solution of *cis*-**10** with visible light (ESI, Figure S41). It is conceivable that a polar solvent, such as THF had weakened the intramolecular hydrogen bonding, which led to slow thermal relaxation. The *cis*- and *trans*- isomers of **10** can be switched reversibly by exposing the THF solution to UV- and visible light, respectively. Similarly, fast thermal relaxation was observed for **10** in MeOH owing to the intermolecular proton transfer between methanol and azo group (data not given).

pH-dependent Photochromic Properties of DTE1 and DTE2

As **DTEs** incorporated with phenolic group are sensitive to pH, it is interesting to study their absorption changes upon deprotonation in basic medium. In this study, the photochromic properties of **DTEs** in MeOH were monitored using absorption spectroscopy before and after addition of aqueous NaOH solution (Figure 6). **DTE1**$_{open}$ and **DTE2**$_{open}$ showed red-shifts in absorption maxima (10 nm) with decrease in absorption intensities after the addition of aqueous NaOH solution (Figure 6a and 6c). The colorless solutions of **DTE1**$_{open}$ and **DTE2**$_{open}$ have immediately turned into yellowish after deprotonation of phenolic group in presence of NaOH (ESI, Figure S42). On the other hand, addition of aqueous NaOH solution to the methanol solutions of **DTE1**$_{closed}$ and **DTE2**$_{closed}$

View Article Online
DOI: 10.1039/C6RA21348K

resulted in red-shifts in absorption maxima (10 nm, Figure 6b and 6d). The color of **DTE1**$_{closed}$ has changed from blue to green upon addition of aqueous NaOH solution, whereas **DTE2**$_{closed}$ showed a dark blue color after deprotonation. The color contrast of **DTE1**$_{closed}$ before and after deprotonation demonstrates potential applications for developing a pH sensor.

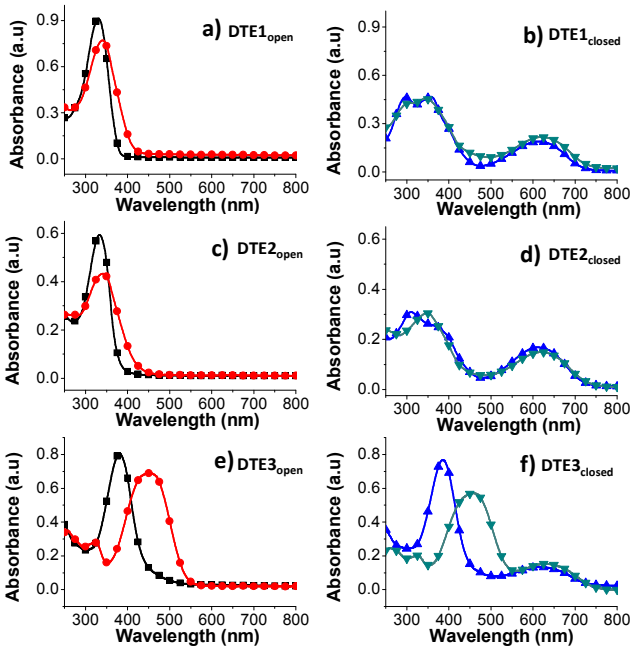

Figure 6. Absorption spectra of **DTE**$_{open}$ solution in MeOH before (-■-) and after (-●-) addition of aqueous NaOH solution; and **DTE**$_{closed}$ solution in MeOH before (-▲-) and after (-▼-) addition of aqueous NaOH solution at room temperature.

pH-dependent Photochromic Properties of DTE3

DTE3 with azophenolic group showed a more significant red-shift in absorption maximum after deprotonation. Appearance of a new absorption maximum at 452 nm for **DTE3**$_{open}$ was observed upon addition of aqueous NaOH solution (Figure 6e), which gave deep orange solution. Similar changes in absorption spectra (red shift of 64 nm) were also observed for **DTE3**$_{closed}$ after addition of aqueous NaOH solution (Figure 6f). However, the photoisomerization of deprotonated **DTE3**$_{open}$ was observed to be slower and required an irradiation time of up to 10 minutes to reach photostationary state in comparison to neutral **DTE3**$_{open}$ (5 minutes).

Photochromic properties of DTEs in presence of Fe^{3+} ions

It is understood that the phenolic compounds have strong affinity towards Fe^{3+} ions. **DTE1**$_{open}$ showed no spectral changes upon addition of Fe^{3+} ions (1 eq) in MeOH (Figure 7a). The absorption peak of **DTE1**$_{closed}$ in presence of Fe^{3+} ions resembles to that of **DTE1**$_{closed}$ in the absence of Fe^{3+} ions, which suggested that Fe^{3+} has negligible effect on **DTE1**$_{open}$ photoisomerization (Figure 7b). In Figure 7c, **DTE2**$_{open}$ exhibited large red-shift in absorption maxima (27 nm) after addition of Fe^{3+} ions in solution, indicating a strong complexation between Fe^{3+} ions and catechol groups of **DTE2**$_{open}$. On the other hand, smaller photoconversion was observed in **DTE2**$_{closed}$ complex as evident from the lower absorbance at 620 nm (Figure 7d). **DTE3**$_{open}$ showed a decrease in intensities of absorption maximum at 382 nm and appearance of a shoulder peak at 460 nm upon addition of Fe^{3+} ions in solution (Figure 7e). In comparison to **DTE1**, **DTE3** showed a strong interaction with Fe^{3+} ions (Figure 7f). It is conceivable that the presence of azo- group influences the interaction with Fe^{3+} ions, which gave large red-shift in absorption maximum.[30]

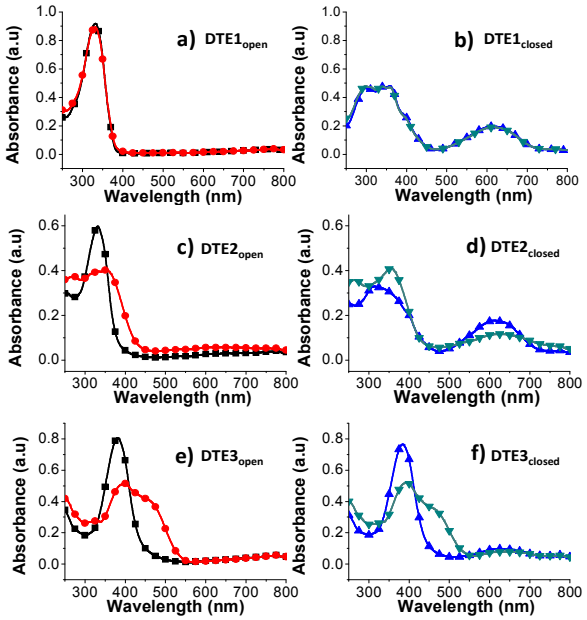

Figure 7. Absorption spectra of **DTE**$_{open}$ solution in MeOH before (-■-) and after (-●-) addition of aqueous Fe^{3+} solution; and **DTE**$_{closed}$ solution in MeOH before (-▲-) and after (-▼-) addition of aqueous Fe^{3+} solution; the ratio of **DTE** : Fe^{3+} used was 1 : 1, and Fe^{3+} ions were added prior to photoisomerization of **DTEs** in presence of K_2CO_3.

Electrochemical Properties of DTEs

The electrochemical properties of **DTEs** were evaluated using cyclic voltammetry (CV) with a platinum working electrode and Ag/AgCl reference electrode, using a solution of 0.1 M tetrabutylammonium hexafluorophosphate in anhydrous dichloromethane and at a scan rate of 100 mVs^{-1} before and after irradiation with UV-light (365 nm, 10 minutes). As shown in Figure 8a, **DTE1**$_{open}$ showed an irreversible oxidation peak at +1.52 V, which corresponds to the oxidation of dithienylethene

View Article Online
DOI: 10.1039/C6RA21348K

group. The electrochemical oxidation has led to formation of **DTE1**$_{closed}$ in solution. The repetitive CV scans resulted in a smaller oxidation peak at + 1.52 V and appearance of a new oxidation peak at + 1.20 V, where the latter was caused by the formation of **DTE1**$_{closed}$. This is confirmed from the CV trace of **DTE1**$_{closed}$ obtained from photoisomerization. Similar electrochemically induced ring-closing reactions have been observed for other dithienylethene derivatives.[31] As shown in Figure 8b, **DTE2**$_{open}$ underwent an irreversible oxidation at around + 1.50 V in the first scan, followed by formation of **DTE2**$_{closed}$ with the appearance of a new oxidation peak at around + 1.17 V in the second scan. This suggests both **DTE1**$_{open}$ and **DTE2**$_{open}$ can be switched electrochemically to **DTE1**$_{closed}$ and **DTE2**$_{closed}$.

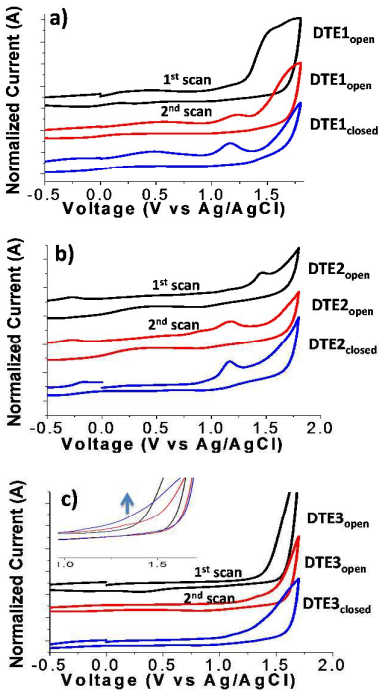

Figure 8. Cyclic voltammograms of **DTE1** (**a**), **DTE2** (**b**), and **DTE3** (**c**) recorded in a 0.1 M solution of tetrabutylammonium hexafluorophosphate in dichloromethane at a scan rate of 100 mVs^{-1} with a Ag/AgCl as a reference electrode. The photoisomerizations of **DTEs** were carried out by irradiating the dichloromethane solutions with UV-light (365 nm, 10 minutes).

In contrast, the electrochemical switching of **DTE3**$_{open}$ is relatively weaker, which showed irreversible oxidations at around + 1.58 V in the first scan. After a few scans, small oxidation peaks were observed for **DTE3**$_{closed}$ at + 1.32 V (Figure 8c), which suggested a weak electrochemical switching of **DTE3** molecules. The CV trace of photochemically switched **DTE3**$_{closed}$ showed no significant difference from the electrochemically switched **DTE3**$_{closed}$.

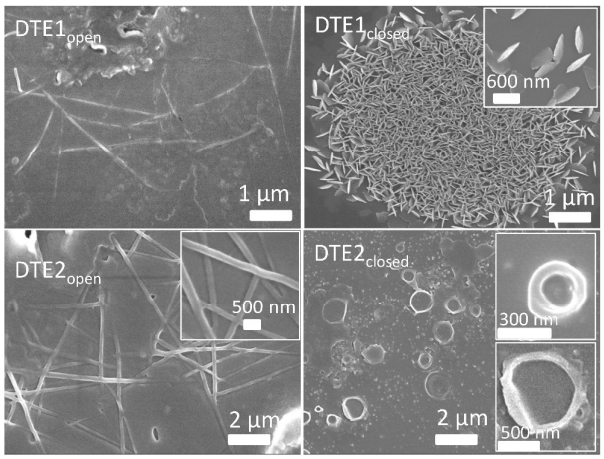

Figure 9. FESEM images of **DTE1** and **DTE2** films from THF solution (6.0 x 10^{-4} M) on precleaned glass substrates. THF was allowed to evaporate slowly inside a desiccator at room temperature under darkness. Films from **DTE1**$_{closed}$ and **DTE2**$_{closed}$ were prepared by irradiating the solution with UV light (365 nm, 10 minutes) prior to drop casting.

Self-assembly of DTE1 and DTE2 in THF

Self-assembly of **DTE1 – 2** was examined using scanning electron microscopy (SEM). Thin films were prepared by drop casting dilute solutions of **DTEs** in THF (6.0 x 10^{-4} M) on glass substrates. **DTE1 – 2**$_{closed}$ films were prepared by irradiating the dilute solution with UV-light (365 nm, 10 minutes) prior to drop casting. Solvent was allowed to evaporate slowly in a desiccator at room temperature under darkness prior to SEM examination. **DTE1**$_{open}$ and **DTE2**$_{open}$ films showed formation of long micrometer-length needles with diameters of 120 to 240 nm (Figure 9) upon slow evaporation of THF at room temperature.

In comparison, **DTE1**$_{closed}$ showed formation of plate-type structures with sizes at around 150 nm. It is conceivable that the increase in rigidity of closed-ring **DTE1** disrupted the self-assembly of molecules into one-dimensional needles. On the other hand, the higher rotational freedoms for **DTE1**$_{open}$ and **DTE2**$_{open}$ and intermolecular interactions such as hydrogen bonding and π - π stacking showed an important role towards the formation of large needles. Nano-sized spheres and donut-like structures with various sizes (300 nm to 2 µm) were formed from **DTE2**$_{closed}$ under identical conditions. The rings were only formed from **DTE2**$_{closed}$ with end catechol groups but not from other molecules, highlighting the importance of multiple intra- and inter- molecular hydrogen bonds towards the formation of circular structures.

View Article Online
DOI: 10.1039/C6RA21348K

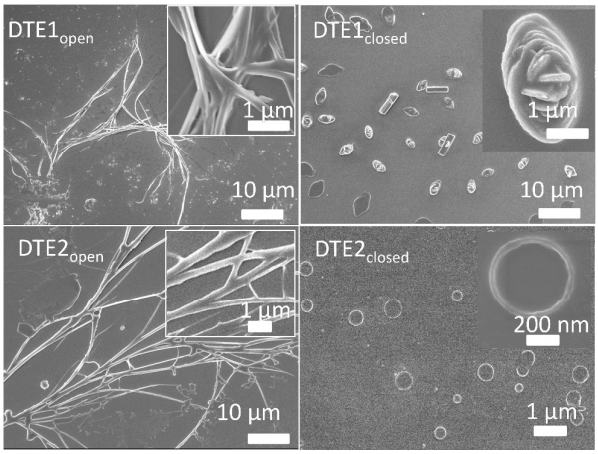

Figure 10. FESEM images of **DTE1** and **DTE2** films drop-casted from MeOH solution (6.0 x 10^{-4} M) on a precleaned glass substrate. MeOH was allowed to evaporate slowly inside a desiccator at room temperature under darkness. **DTE1**$_{closed}$ and **DTE2**$_{closed}$ films were prepared by first irradiating the solution with UV light (365 nm, 10 minutes) prior to drop casting.

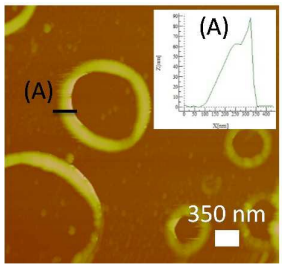

Figure 11. AFM image (tapping mode) and the height profiles of **DTE2**$_{closed}$ rings on silicon substrate. The **DTE2**$_{closed}$ solution (365 nm, 10 minutes) in MeOH (6.0 x 10^{-4} M) was drop-casted on a pre-cleaned silicon substrate and the solvent was allowed to evaporate slowly at room temperature under darkness. Inset: the thickness (x-axis) and height (y-axis) of the **DTE2**$_{closed}$ rings were determined to be in the range of 160 – 250 nm, and 55 – 90 nm, respectively.

Self-assembly of DTE1 and DTE2 in MeOH

Thin films of **DTE1** – **2** prepared from methanol solutions were also examined in order to understand the solvent effects on the self-assembly of **DTEs** (Figure 10). Long needles (length ~100 µm) of **DTE1**$_{open}$ and **DTE2**$_{open}$ were obtained from MeOH. Similarly, **DTE1**$_{closed}$ film showed micron-sized crystalline structures and **DTE2**$_{closed}$ gave smaller circular structures with diameters in the range of 300 – 600 nm. **DTE2**$_{open}$ needles were irradiated at 365 nm prior to SEM examination. However, no transformation of assembled structures was observed. It is conceivable that the structural changes of **DTE2** in solid state are difficult as compared to that in solution state.

Atomic force microscopy (AFM) was used to measure the thickness and the height of ring-shaped nanostructures of **DTE2**$_{closed}$ formed on a silicon substrate (Figure 11). The **DTE2** solution in MeOH was irradiated with UV light (365 nm, 10 minutes) prior to dropcasting. The thickness and height of ring-shaped nanostructures were determined to be in the range of 160 – 250 nm, and 55 – 90 nm, respectively. Formation of nanorings with a diameter of 150 nm were also reported from polyfluorene by using water droplet as template.[32]

It is also known that coffee ring formations are commonly observed from slow evaporation of liquid containing dispersed particles on the surface.[33] However, smallest coffee rings reported were in the size range of 8 – 10 µm,[34, 35] which are much larger than the observed circular nanostructures from this work. Moreover, the capillary flow that causes the non-uniform deposition of particles in the coffee rings was suppressed by organic solvents such as ethanol, methanol, octane and THF with strong Marangoni effect,[36] which induced convection flow and resulted in uniform depositions.[37] In addition, the self-assembly of **DTE2** are controllable from one dimensional micro-sized needle in open-ring isomer to circular nanostructures in closed-ring isomer. Therefore, the self-assembly mechanism for **DTE2** is different from that of the coffee ring formation.

In an effort to further understand the mechanism of the formation of circular nanostructures in **DTE2**$_{closed}$, deprotonation of **DTE2**$_{closed}$ (6.0 x 10^{-4} M) was carried out by using NaOH (4 eq) in MeOH. It is found that the deprotonated **DTE2**$_{closed}$ film showed random shaped aggregates with no observable circular or needle-like structures (ESI, Figure S43). It is proposed that the formation of circular nanostructures in **DTE2**$_{closed}$ involved an interplay of both inter/intramolecular hydrogen bonding and rigidity of the molecular structure of closed dithienylethene group (Figure 12). The **DTE2**$_{closed}$ molecules are connected via intermolecular hydrogen bonding, while the rigid dithienylethene backbone of **DTE2**$_{closed}$ could provide a "bent" conformation that leads to circular nanostructures. The self-assembly of macrocyclic triazolophanes into nano-sized toroids and donuts, which involved both hydrogen bonds and rigid macromolecules was reported recently.[38]

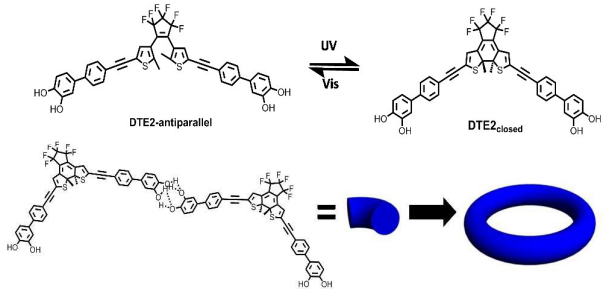

Figure 12. The photoinduced ring-closing of **DTE2** happens when it is in antiparallel conformation; Schematic representation of possible mechanism for **DTE2**$_{closed}$ self-assembly via inter/intra-molecular hydrogen bonding between end catechol groups.

View Article Online
DOI: 10.1039/C6RA21348K

Self-assembly of DTE3

DTE3$_{open}$ film cast from MeOH (6.0 x 10^{-4} M) showed random-shaped aggregates in the micron size range (ESI, Figure S44), which is morphologically different from the **DTE1**$_{open}$ without azo group. **DTE3**$_{open}$ film cast from THF (6.0 x 10^{-4} M) showed random-shaped structures with smooth and featureless surfaces. In contrast, **DTE3**$_{closed}$ film showed well-defined needle structures, which indicate that the assembly of **DTE3** is dependent on the structural changes by photocyclization.

Conclusions

In this work, dithienylethene based photochromic compounds with phenols (**DTE1**), catechols (**DTE2**), azophenols (**DTE3**) as end groups were synthesized. All target molecules showed solvent dependent photochromic properties owing to the photoinduced transition between closed-ring and open-ring isomers of dithienylethene. The photoconversion yields of **DTE3** (32%) are smaller than that of **DTE1** - **2** (70 – 74%) due to a fast thermal relaxation of *cis*-azophenols to *trans*-azophenols upon photoisomerization in chloroform. In contrast, both closed-ring dithienylethene and *cis*-azophenols (*cis*-**DTE3**$_{closed}$) were observed in THF owing to a better thermal stability of *cis*-azophenols in THF. The transition from needle microstructures to circular nanostructures with diameters in the range of 300 – 600 nm was observed for **DTE2** film upon ring-closing of dithienylethene unit, which could be used for developing interesting optical materials.

Experimental

Materials

The dithienylperfluorocyclopentene (**DTE**) was prepared according to the previously reported procedures.[39, 40] All reagents and solvents were purchased from commercial sources (Sigma Aldrich, Alfa Aesar and Merck) and used without further purification. Preparative separations were performed by column chromatography on a silica gel grade 60 (0.040 – 0.063 mm) from Silicycle.

Instrumentation

^{1}H NMR and ^{13}C NMR spectra were recorded on a Bruker Avance AV300 (300 MHz), or a Bruker Avance AV500 (500 MHz) NMR instruments using appropriate deuterated solvents purchased from Cambridge Isotope Laboratories. The chemical shifts were reported in part per million or ppm and referenced to the residual solvent peak: s = singlet, d = doublet, t = triplet, m = multiplet, and b = broad. Electron Impact mass spectroscopy (EI–MS) mass spectra were obtained on a Finnigan TSQ7000. Atmospheric pressure chemical ionization (APCI) mass spectra were obtained on a Bruker AmaZonX. Elemental analysis was carried out on Elementar Vario Micro Cube. Absorption spectra were measured on a UV-1800 Shimadzu UV-VIS spectrophotometer with an optical filter calibrated at a bandwidth of 1 nm. The emission spectra were measured on a RF-5301PC Shimadzu spectrofluorophotometer. The cyclic voltammograms were recorded with a computer controlled CHI electrochemical analyzer at a constant scan rate of 100 mV/s. Scanning Electron micrograph was recorded on a JEOL JSM-6701F Field Emission Scanning Electron Microscope (SEM). **DTE1-3** were dissolved in respective solvents (THF and MeOH), followed by drop-casting on a precleaned glass substrate, and solvent was allowed to evaporate at 25 ºC under ambient conditions. Atomic Force Microscope (AFM) measurements were recorded using a Agilent Technologies AFM Picoscan 5 instrument.

Synthesis Procedures

Compound 1 : A solution of 4-iodoanisole (1.08 g, 4.6 mmol), 4-bromophenylboronic acid (1.2 g, 5.98 mmol) and bis(triphenylphosphine)palladium(II) (0.16 g, 0.22 mmol) in tetrahydrofuran/Aliquat® 336/2M aqueous K_2CO_3 solution (12 : 2 : 5 mL) was stirred at reflux temperature for overnight, cooled, diluted with ethyl acetate (50 mL), washed with water (2 x 15 mL) and brine solution (10 mL). The organic layer was dried over anhydrous sodium sulfate and the excess solvent was removed under reduced pressure. The crude product was purified on a silica gel column using 5% dichloromethane in hexane as eluent to afford a white solid (1.01 g, yield 83%). ^{1}H NMR (300 MHz, $CDCl_3$) δ 7.53 (d, *J* = 8.6 Hz, 2H), 7.49 (d, *J* = 8.9 Hz, 2H), 7.41 (d, *J* = 8.6 Hz, 2H), 6.97 (d, *J* = 8.9 Hz, 2H). ^{13}C NMR (126 MHz, $CDCl_3$) δ 159.46, 139.78, 132.54, 131.79, 128.30, 127.98, 120.79, 114.36, 55.36. HR-MS (EI): M^+ ($C_{13}H_{11}BrO$) Calculated m/z =261.9993, Found m/z = 261.9992. Elemental analysis calculated (%) for $C_{13}H_{11}BrO$: C, 59.34; H, 4.21; Found: C, 59.14; H, 4.28.

Compound 2: Compound **1** (0.42 g, 1.59 mmol) was dissolved in anhydrous dichloromethane (14 mL) under nitrogen atmosphere. The reaction mixture was cooled to -50 °C followed by dropwise addition of BBr_3 (0.31 mL, 3.26 mmol). The reaction mixture was warmed up to room temperature, stirred for 3 hours, and quenched with water (10 mL). The organic layer was washed with water (2 x 5 mL) and brine solution (3 mL), dried over anhydrous sodium sulfate, filtered, and the excess solvent was removed under reduced pressure. The crude product was purified on a silica gel column using a mixture of 10% ethyl acetate in hexane as eluent to afford a white solid (0.36 g, yield 90%). ^{1}H NMR (300 MHz, $CDCl_3$) δ 7.53 (d, J = 8.6 Hz, 2H), 7.43 (d, J = 8.7 Hz, 2H), 7.39 (d, J = 8.6 Hz, 2H), 6.90 (d, *J* = 8.7 Hz, 1H), 4.84 (br, 1H). ^{13}C NMR (75 MHz, $CDCl_3$) δ 155.39, 139.67, 132.75, 131.78, 128.28, 128.22, 120.83, 115.77. HR-MS (EI): M^+ ($C_{12}H_9BrO$) Calculated m/z =247.9836, Found m/z = 247.9838. Elemental analysis calculated (%) for $C_{12}H_9BrO$: C, 57.86; H, 3.64; Found: C, 57.91; H, 3.63.

Compound 3: A solution of Compound **2** (0.32 g, 1.28 mmol), tetrakis(triphenylphosphine)palladium(0) (0.074 g, 0.06 mmol) and copper(I) iodide (0.02g, 0.10 mmol) in tetrahydrofuran/triethylamine (6 : 6 mL) was stirred at room temperature under nitrogen atmosphere. Ethynyltrimethylsilane (0.55 mL, 3.89 mmol) was added via

View Article Online
DOI: 10.1039/C6RA21348K

syringe and the reaction mixture was stirred at 80 °C for 24 hours, cooled, and the excess solvent was removed under reduced pressure. The residue solid was purified on a silica column using a mixture of 10% ethyl acetate in hexane to afford a white solid, which was dissolved in tetrahydrofuran (5 mL) and cooled to 0 °C. Tetrabutylammonium fluoride (2.5 mL, 2.5 mmol, 1 M in tetrahydrofuran) was added dropwise and the reaction mixture was stirred at 0 °C for 30 minutes. The reaction mixture was diluted with ethyl acetate (20 mL), washed with water (2 x 10 mL) and brine solution (5 mL), dried over anhydrous sodium sulfate, and the excess solvent was removed under reduced pressure. The crude product was purified on a silica gel column using a mixture of 10% ethyl acetate in hexane as eluent to afford a white solid (0.20 g, yield 80%). ^{1}H NMR (300 MHz, $CDCl_3$) δ 7.50 (m, 4H), 7.48 (d, *J* = 8.6 Hz, 2H), 6.91 (d, *J* = 8.6 Hz, 2H), 4.88 (br, 1H), 3.11 (s, 1H). ^{13}C NMR (126 MHz, $CDCl_3$) δ 155.48, 141.10, 132.97, 132.52, 128.33, 126.47, 120.31, 115.76, 83.63, 77.51. HR-MS (EI): M^+ ($C_{14}H_{10}O$) Calculated m/z =194.0731, Found m/z = 194.0736. Elemental analysis calculated (%) for $C_{14}H_{10}O$: C, 86.57; H, 5.19; Found: C, 85.99; H, 5.15.

Compound 4: 4-Bromo-1,2-dimethoxybenzene (1.00 g, 4.6 mmol), bis(pinacolato)diboron (1.51 g, 5.95 mmol), $PdCl_2$(dppf) (0.22 g, 0.27 mmol) and potassium acetate (0.45 g, 4.6 mmol) were dissolved in 1,4-dioxane (30 mL) under nitrogen atmosphere. The reaction mixture was stirred at 80 °C for overnight, cooled, added with water (20 mL), and the product was extracted with ethyl acetate (2 x 30 mL). The combined organic layer was washed with water (2 x 15 mL) and brine solution (10 mL), dried over anhydrous sodium sulfate, and the excess solvent was removed under reduced pressure. The crude product was purified on a silica gel column using a mixture of 5% ethyl acetate in hexane as eluent to afford a sticky colorless liquid (1.03 g, yield 85%). ^{1}H NMR (300 MHz, $CDCl_3$) δ 7.43 (d, *J* = 8.0 Hz, 1H), 7.29 (s, 1H), 6.88 (d, *J* = 8.0 Hz, 1H), 3.92 (s, 3H), 3.90 (s, 3H), 1.34 (s, 12H). ^{13}C NMR (75 MHz, $CDCl_3$) δ 151.65, 148.35, 128.55, 116.59, 110.50, 83.64, 55.84, 55.73, 25.00, 24.84. HR-MS (EI): M^+ ($C_{14}H_{21}BO_4$) Calculated m/z =264.1533, Found m/z = 264.1523. Elemental analysis calculated (%) for $C_{14}H_{21}BO_4$: C, 63.66; H, 8.01; Found: C, 63.89; H, 8.01.

Compound 5: The synthesis and work-up of **5** were same as described for Compound **1**. Compound **4** (1.2 g, 4.54 mmol), 1-bromo-4-iodobenzene (1.4 g, 4.95 mmol), bis(triphenylphosphine)palladium(II) (0.16 g, 0.22 mmol) were reacted in tetrahydrofuran/Aliquat® 336/2M aqueous K_2CO_3 solution (12 : 2 : 5 mL) as solvent. The crude solid was purified on silica gel column using a mixture of 5% ethyl acetate in hexane as eluent to afford a white solid (1.05 g, yield 79%). ^{1}H NMR (300 MHz, $CDCl_3$) δ 7.54 (d, *J* = 8.6 Hz, 2H), 7.42 (d, *J* = 8.6 Hz, 2H), 7.14 – 7.03 (m, 2H), 6.94 (d, *J* = 8.3 Hz, 1H), 3.95 (s, 3H), 3.92 (s, 3H). ^{13}C NMR (75 MHz, $CDCl_3$) δ 149.24, 148.89, 139.94, 132.94, 131.78, 128.41, 120.94, 119.28, 111.51, 110.16, 55.98. HR-MS (EI): M^+ ($C_{14}H_{13}BrO_2$) Calculated m/z =292.0099, Found m/z = 292.0094. Elemental analysis calculated (%) for $C_{14}H_{13}BrO_2$: C, 57.36; H, 4.47; Found: C, 58.01; H, 4.53.

Compound 6: The synthesis and work-up of **6** were same as described for Compound **2**.
Compound **5** (0.74 g, 2.52 mmol) and BBr_3 (0.72 mL, 7.59 mmol) were reacted in anhydrous dichloromethane (20 mL) as solvent. The crude solid was purified on a silica gel column using a mixture of 30% ethyl acetate in hexane as eluent to afford a white solid (0.56 g, yield 84%). ^{1}H NMR (300 MHz, $CDCl_3$) δ 7.52 (d, *J* = 8.6 Hz, 2H), 7.38 (d, *J* = 8.6 Hz, 2H), 7.10 – 6.98 (m, 2H), 6.92 (d, *J* = 8.2 Hz, 1H), 5.26 (s, 2H). ^{13}C NMR (126 MHz, $CDCl_3$) δ 143.88, 143.39, 139.59, 133.51, 131.79, 128.32, 120.98, 119.70, 115.80, 114.08. HR-MS (EI): M^+ ($C_{12}H_9BrO_2$) Calculated m/z =263.9786, Found m/z = 263.9776. Elemental analysis calculated (%) for $C_{12}H_9BrO_2$: C, 54.37; H, 3.42; Found: C, 54.45; H, 3.33.

Compound 7: The synthesis and work-up of **7** were same as described for **3**.
Compound **6** (0.46 g, 1.74 mmol), tetrakis(triphenylphosphine)palladium(0) (0.11 g, 0.095 mmol), copper(I) iodide (0.026 g, 0.136 mmol), and ethynyltrimethylsilane (1.2 mL, 8.68 mmol) were reacted in tetrahydrofuran/triethylamine (6 : 6 mL). The crude solid was purified on a silica gel column using a mixture of 20% ethyl acetate in hexane as eluent to afford the pale-yellow solid, which was dissolved in tetrahydrofuran (10 mL) followed by addition of tetrabutylammonium fluoride (3.5 mL, 3.47 mmol). The crude product was purified on a silica gel column using a mixture of 20% ethyl acetate in hexane as eluent to afford a white solid (0.25 g, yield 69%). ^{1}H NMR (300 MHz, $CDCl_3$) δ 7.56 – 7.34 (m, 4H), 7.14 – 6.98 (m, 2H), 6.93 (d, *J* = 8.2 Hz, 1H), 5.23 (s, 2H), 3.11 (s, 1H). ^{13}C NMR (75 MHz, $CDCl_3$) δ 143.85, 133.76, 132.52, 131.79, 128.32, 126.54, 119.89, 115.81, 114.19. HR-MS (EI): M^+ ($C_{14}H_{10}O_2$) Calculated m/z =210.0680, Found m/z = 210.0676. Elemental analysis calculated (%) for $C_{14}H_{10}O_2$: C,79.98; H, 4.79; Found: C, 80.79; H, 4.75.

Compound 10: The synthesis and work-up of **10** were same as described for **3**.
Compound **8** (1.2 g, 4.33 mmol), tetrakis(triphenylphosphine)palladium(0) (0.48 g, 0.42 mmol), copper(I) iodide (0.08 g, 0.42 mmol), and ethynyltrimethylsilane (0.92 mL, 6.5 mmol) were reacted in tetrahydrofuran/triethylamine (10 : 10 mL). The crude solid was purified on a silica gel column using a mixture of 15% ethyl acetate in hexane as eluent to afford the brown solid, which was dissolved in tetrahydrofuran (10 mL) followed by addition of tetrabutylammonium fluoride (8.6 mL, 8.64 mmol). The crude product was purified on a silica gel column using a mixture of 15 % ethyl acetate in hexane as eluent to afford a brown solid (0.78 g, 81%). ^{1}H NMR (300 MHz, $CDCl_3$) δ 7.89 (d, *J* = 8.8 Hz, 2H), 7.84 (d, *J* = 8.4 Hz, 2H), 7.62 (d, *J* = 8.4 Hz, 2H), 6.96 (d, *J* = 8.8 Hz, 2H), 3.21 (s, 1H). ^{13}C NMR (75 MHz, $CDCl_3$) δ 158.66, 152.22, 147.10, 132.94, 125.19, 123.98, 122.53, 115.88, 83.32, 79.12. Elemental analysis calculated (%) for

View Article Online
DOI: 10.1039/C6RA21348K

$C_{14}H_{10}N_2O$: C,75.66; H, 4.54; N, 12.60; Found: C, 74.99; H, 4.45; N, 11.90.

DTE1

A solution of **DTE** (0.20 g, 0.32 mmol), **3** (0.13 g, 0.67 mmol), tetrakis(triphenylphosphine)palladium(0) (0.014 g, 0.012 mmol), and copper(I) iodide (4.5 mg, 0.023 mmol) in a mixture of tetrahydrofuran/diisopropylamine (8 : 4 mL) was stirred at 80 °C for overnight under nitrogen atmosphere, cooled, and the excess solvent was removed under reduced pressure. The residue was purified on a silica gel column using a mixture of 50% ethyl acetate in hexane as eluent to afford a pale-yellow solid (0.12 g, yield 49%). ^{1}H NMR (300 MHz, CD_2Cl_2) δ 7.60 (s, 8H), 7.55 (d, *J* = 8.7 Hz, 4H), 7.32 (s, 2H), 6.96 (d, *J* = 8.7 Hz, 4H), 5.17 (s, 2H), 2.01 (s, 6H). ^{13}C NMR (126 MHz, CD_2Cl_2) δ 156.15, 144.12, 141.33, 132.94, 132.10, 131.64, 128.56, 126.86, 125.09, 122.30, 120.90, 116.08, 94.17, 82.12, 14.67. HRMS (APCl, +ve, $(M+H)^+$) : ($C_{43}H_{27}F_6O_2S_2$) Calculated *m/z* = 753.1345, Found *m/z* = 753.1351. Elemental analysis calculated (%) for $C_{43}H_{26}F_6O_2S_2$: C, 68.61; H, 3.48; S, 8.52; Found: C, 68.72; H, 3.55; S, 8.67.

DTE2

The synthesis of **DTE2** was same as described for **DTE1**.

A solution of **DTE** (0.21 g, 0.34 mmol), **7** (0.17 g, 0.80 mmol), tetrakis(triphenylphosphine)palladium(0) (0.019 g, 0.016 mmol), and copper(I) iodide (3.9 mg, 0.020 mmol) in a mixture of tetrahydrofuran/diisopropylamine (8 : 4 mL) was stirred at 80 °C for overnight under nitrogen atmosphere, cooled, and the excess solvent was removed under reduced pressure. The residue was purified on a silica gel column using a mixture of 60% ethyl acetate in hexane as eluent to afford a pale-yellow solid (0.09 g, yield 34%). ^{1}H NMR (300 MHz, $CDCl_3$) δ 7.53 (s, 8H), 7.14 (s, 4H), 7.08 (d, *J* = 8.2 Hz, 2H), 6.94 (d, *J* = 8.2 Hz, 2H), 5.36 (s, 4H), 1.97 (s, 6H). ^{13}C NMR (75 MHz, MeOD) δ 146.82, 145.01, 143.17, 133.84, 133.28, 132.84, 132.24, 129.92, 127.51, 126.04, 123.64, 121.45, 119.59, 116.87, 114.93, 95.21, 82.14, 14.49. HRMS (APCl, +ve, $(M+H)^+$) : ($C_{43}H_{27}F_6O_4S_2$) Calculated *m/z* = 785.1249, Found *m/z* = 785.1242. Elemental analysis calculated (%) for $C_{43}H_{26}F_6O_4S_2$: C, 65.81; H, 3.34; S, 8.17; Found: C, 66.11; H, 3.34; S, 7.99.

DTE3

The synthesis of **DTE3** was same as described for **DTE1**.

A solution of **DTE** (0.1 g, 0.16 mmol), **10** (0.29 g, 0.35 mmol), tetrakis(triphenylphosphine)palladium(0) (0.037 g, 0.032 mmol), and copper(I) iodide (0.006 g, 0.032 mmol) in a mixture of tetrahydrofuran/diisopropylamine (8 : 4 mL) was stirred at 80 °C for overnight under nitrogen atmosphere, cooled, and the excess solvent was removed under reduced pressure. The residue was purified on a silica gel column using a mixture of 40% ethyl acetate in hexane as eluent to afford a red solid (0.10 g, yield 79%). ^{1}H NMR (300 MHz, $CDCl_3$) δ 7.90 (d, *J* = 6.0 Hz, 4H), 7.87 (d, *J* = 6.0 Hz, 4H), 7.63 (d, *J* = 8.8 Hz, 4H), 7.30 (s, 2H), 6.96 (d, *J* = 8.8 Hz, 4H), 1.97 (s, 6H). ^{13}C NMR (75 MHz, $CDCl_3$) δ 158.59, 152.13, 147.23, 143.76, 132.20, 131.66, 125.21, 124.93, 124.37, 122.73, 121.66, 115.88, 93.95, 83.58, 14.53. HRMS (APCl): calculated for $C_{43}H_{26}F_6N_4O_2S_2$ $(M)^+$ *m/z* 808.1396, found *m/z* 808.1397. Elemental analysis calculated (%) for $C_{43}H_{26}F_6N_4O_2S_2$: C, 63.86; H, 3.24; N, 6.93; S: 7.93; Found: C, 64.53; H, 3.31; N, 7.01; S, 7.69.

Sample preparation for photophysical studies of DTEs

Dilute solutions of **DTEs** were prepared by dissolving appropriate amount of **DTEs** in analytical grade solvents. The concentrations for **DTE1**, **DTE2**, and **DTE3** were 4.8 x 10^{-5} M, 2.5 x 10^{-5} M, and 0.8 x 10^{-5} M, respectively. The quartz cuvette with optical path length of 1 cm was used. For thin films studies, the **DTEs** solutions in analytical grade solvent were drop-casted on quartz plates and the solvent was allowed to evaporate under ambient conditions.

Sample preparation for photophysical studies of DTEs at different pHs

Dilute solutions of **DTEs** were prepared by dissolving appropriate amount of **DTEs** in analytical grade solvents. The concentrations for **DTE1**, **DTE2**, and **DTE3** were 5.0 x 10^{-5} M, 2.5 x 10^{-5} M, and 2.2 x 10^{-5} M, respectively. The quartz cuvette with optical path length of 1 cm was used. Aqueous NaOH solution (1.0 x 10^{-5} M) was added to the **DTEs** solutions before or after irradiation with UV light at 365 nm, prior to spectroscopic analyses. Next, dilute aqueous HCl solution was added to neutralize the **DTEs** solutions to test the reversibility of the optical spectra.

Sample preparation for photophysical studies of DTEs in presence of Fe^{3+} ions

Dilute solutions of **DTEs** were prepared by dissolving appropriate amount of **DTEs** in analytical grade solvents. The concentrations for **DTE1**, **DTE2**, and **DTE3** were 5.0 x 10^{-5} M, 2.5 x 10^{-5} M, and 2.2 x 10^{-5} M, respectively. The quartz cuvette with optical path length of 1 cm was used. Aqueous $Fe(NO_3)_3$ solution (1 equivalent) was added to the **DTEs** solutions before or after irradiation with UV light at 365 nm in presence of K_2CO_3, prior to spectroscopic analyses.

Sample preparation for electrochemical studies

Dilute solutions of **DTEs** were prepared by dissolving appropriate amount of **DTEs** in anhydrous dichloromethane (0.5 mg/mL), which was distilled from calcium hydride under nitrogen atmosphere. The cyclic voltammograms of DTEs were recorded in a 0.1 M solution of tetrabutylammonium hexafluorophosphate in dichloromethane at a scan rate of 100 mV s^{-1}, with a Ag/AgCl as reference electrode, platinum wire as counter electrode, and platinum disk as working electrode.

Sample preparation for morphology studies

Dilute solutions of **DTEs** were prepared by dissolving appropriate amount of **DTEs** in analytical grade solvents. The concentration for all **DTEs** solutions was 6.0 x 10^{-4} M. 20 µL of the **DTEs** solution was pipetted and drop-casted on glass substrates and the solvent was allowed to evaporate slowly in a desiccator under ambient conditions under darkness for 24 hours. $\mathbf{DTE1}_{closed}$ and $\mathbf{DTE2}_{closed}$ films were prepared by first

View Article Online
DOI: 10.1039/C6RA21348K

irradiating the solution with UV light (365 nm, 10 minutes) prior to drop casting.

Acknowledgements

The authors would like to thank Ministry of Education (MOE), Singapore for funding support (R-143-000-570-112), Department of Chemistry, National University of Singapore (NUS) for technical supports. CPS is grateful for the research graduate scholarship from MOE and NUS.

Notes and references

1. M. Qin, Y. Huang, F. Li and Y. Song, *J. Mater. Chem. C*, 2015, **3**, 9265-9275.
2. C. Zheng, S. Pu, G. Liu, B. Chen and Y. Dai, *Dyes Pigments*, 2013, **98**, 280-285.
3. D. Gust, J. Andreasson, U. Pischel, T. A. Moore and A. L. Moore, *Chem. Commun.*, 2012, **48**, 1947-1957.
4. M. D. Manrique-Juárez, S. Rat, L. Salmon, G. Molnár, C. M. Quintero, L. Nicu, H. J. Shepherd and A. Bousseksou, *Coordin. Chem. Rev.*, 2016, **308**, 395-408.
5. H. M. D. Bandara and S. C. Burdette, *Chem. Soc. Rev.*, 2012, **41**, 1809-1825.
6. V. V. Jerca, F. A. Jerca, I. Rau, A. M. Manea, D. M. Vuluga and F. Kajzar, *Opt. Mater.*, 2015, **48**, 160-164.
7. G. Angelini, N. Canilho, M. Emo, M. Kingsley and C. Gasbarri, *J. Org. Chem.*, 2015, **80**, 7430-7434.
8. J. Garcia-Amorós and D. Velasco, *Beilstein J. Org. Chem.*, 2012, **8**, 1003-1017.
9. J. Garcia-Amorós, S. Nonell and D. Velasco, *Chem. Commun.*, 2011, **47**, 4022-4024.
10. C.-T. Poon, W. H. Lam, H.-L. Wong and V. W.-W. Yam, *Chem. Eur. J.*, 2015, **21**, 2182-2192.
11. H. Logtenberg and W. R. Browne, *Org. Biomol. Chem.*, 2013, **11**, 233-243.
12. C. Li, H. Yan, L.-X. Zhao, G.-F. Zhang, Z. Hu, Z.-L. Huang and M.-Q. Zhu, *Nat. Commun.*, 2014, **5**, 5709.
13. X. Cai, L. Zhu, S. Bao and Q. Luo, *Dyes Pigments*, 2015, **121**, 227-234.
14. Y. He, Y. Zhu, Z. Chen, W. He and X. Wang, *Chem. Commun.*, 2013, **49**, 5556-5558.
15. L. Li, F. Q. Bai and H. X. Zhang, *Spectrochim. Acta Mol. Biomol. Spectrosc.*, 2015, **137**, 987-994.
16. S. Yagai, K. Iwai, T. Karatsu and A. Kitamura, *Angew. Chem.*, 2012, **124**, 9817-9821; *Angew. Chem. Int. Ed.*, 2012, **51**, 9679-9683
17. S. Yagai, K. Iwai, M. Yamauchi, T. Karatsu, A. Kitamura, S. Uemura, M. Morimoto, H. Wang and F. Würthner, *Angew. Chem.*, 2014, **126**, 2640-2644; *Angew. Chem. Int. Ed.*, 2014, **53**, 2602–2606.
18. K. Higashiguchi, G. Taira, J.-I. Kitai, T. Hirose and K. Matsuda, *J. Am. Chem. Soc.*, 2015, **137**, 2722-2729.
19. S. Yagai, K. Ishiwatari, X. Lin, T. Karatsu, A. Kitamura and S. Uemura, *Chem. Eur. J.*, 2013, **19**, 6971-6975.
20. X. Cao, J. Zhou, Y. Zou, M. Zhang, X. Yu, S. Zhang, T. Yi and C. Huang, *Langmuir*, 2011, **27**, 5090-5097.
21. A. S. Castanet, F. Colobert, J. R. Desmurs and T. Schlama, *J. Mol. Catal. A: Chem.*, 2002, **182**, 481-487.
22. K. Sonogashira, *J. Organomet. Chem.*, 2002, **653**, 46-49.
23. J. Figueras, *J. Am. Chem. Soc.*, 1971, **93**, 3255-3263.
24. J. Ern, A. T. Bens, H. D. Martin, S. Mukamel, D. Schmid, S. Tretiak, E. Tsiper and C. Kryschi, *Chem. Phys.*, 1999, **246**, 115-125.
25. M. Irie, T. Lifka, S. Kobatake and N. Kato, *J. Am. Chem. Soc.*, 2000, **122**, 4871-4876.
26. Z. Li, J. Yin, X. Wu, Y. Lin, Q. Zeng, F. Fan and S. H. Liu, *J. Photochem. Photobiol. A Chem.*, 2011, **218**, 192-198.
27. H. M. Xiong, Z. D. Wang and Y. Y. Xia, *Adv. Mater.*, 2006, **18**, 748-751.
28. J. Garcia-Amorós, A. Sánchez-Ferrer, W. A. Massad, S. Nonell and D. Velasco, *Phys. Chem. Chem. Phys.*, 2010, **12**, 13238-13242.
29. E. Merino and M. Ribagorda, *Beilstein J. Org. Chem.*, 2012, **8**, 1071-1090.
30. A. Misra and M. Shahid, *J. Phys. Chem. C*, 2010, **114**, 16726-16739.
31. W. R. Browne, J. J. D. D. Jong, T. Kudernac, M. Walko, L. N. Lucas, K. Uchida, J. H. V. Esch and B. L. Feringa, *Chem. Eur. J.*, 2005, **11**, 6414-6429.
32. Y. Liu, T. Murao, Y. Nakano, M. Naito and M. Fujiki, *Soft Matter*, 2008, **4**, 2396-2401.
33. R. D. Deegan, O. Bakajin, T. F. Dupont, G. Huber, S. R. Nagel and T. A. Witten, *Nature*, 1997, **389**, 827-829.
34. X. Shen, C.-M. Ho and T.-S. Wong, *J. Phys. Chem. B*, 2010, **114**, 5269-5274.
35. J. Wu, J. Xia, W. Lei and B.-P. Wang, *RSC Adv.*, 2013, **3**, 5328-5331.
36. H. Hu and R. G. Larson, *J. Phys. Chem. B*, 2006, **110**, 7090-7094.
37. M. Majumder, C. S. Rendall, J. A. Eukel, J. Y. L. Wang, N. Behabtu, C. L. Pint, T.-Y. Liu, A. W. Orbaek, F. Mirri, J. Nam, A. R. Barron, R. H. Hauge, H. K. Schmidt and M. Pasquali, *J. Phys. Chem. B*, 2012, **116**, 6536-6542.
38. V. Haridas, A. R. Sapala and J. P. Jasinski, *Chem. Commun.*, 2015, **51**, 6905-6908.
39. A. K. C. Mengel, B. He and O. S. Wenger, *J. Org. Chem.*, 2012, **77**, 6545-6552.
40. S. Fraysse, C. Coudret and J.-P. Launay, *Eur. J. Inorg. Chem.*, 2000, **2000**, 1581-1590.

View Article Online
DOI: 10.1039/C6RA21348K

Journal Name

ARTICLE

Solvent Dependent Isomerization of Photochromic Dithienylethenes: Synthesis, Photochromism, and Self-assembly.

Choong Ping Sen and Suresh Valiyaveettil*

Department of Chemistry, National University of Singapore.
3 Science Drive 3, Singapore 117543.
Email: chmsv@nus.edu.sg

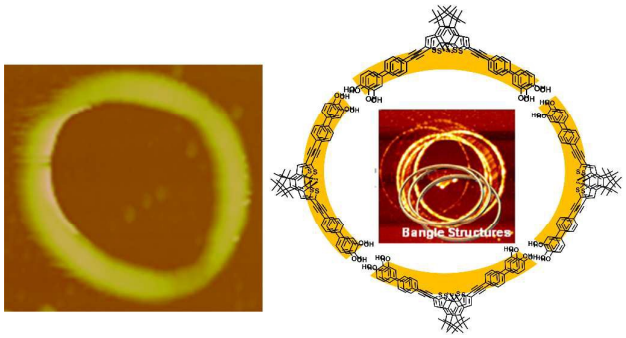

Dithienylethene molecules incorporated with phenolic or azophenolic groups are synthesized and characterized. Self-assembly of circular nanostructures are observed from dithienylethene with catechol end groups. The formation of nanostructures is dependent on factors such as photoisomerization and hydrogen bonding.